Velocity calibration and wavefield decomposition for walkover VSP data

Markus von Steht and Jürgen Mann

Wave Inversion Technology Consortium
Geophysical Institute, University of Karlsruhe (TH)

June 12, 2008

Overview

Theory

CRS approach for VSP geometry
FO CRS traveltime approximation
Calibration method

Data example

Survey description
Velocity calibration
Wavefield decomposition

Conclusions & outlook

CRS approach for VSP geometry

CRS approach for VSP geometry

Finite-offset (FO) 2D CRS stack theory initially introduced for surface seismic (Zhang et al., 2001)

CRS approach for VSP geometry

Finite-offset (FO) 2D CRS stack theory initially introduced for surface seismic (Zhang et al., 2001)

- second order approximation based on paraxial ray-theory

CRS approach for VSP geometry

Finite-offset (FO) 2D CRS stack theory initially introduced for surface seismic (Zhang et al., 2001)

- second order approximation based on paraxial ray-theory
- central ray is non-zero offset

CRS approach for VSP geometry

Finite-offset (FO) 2D CRS stack theory initially introduced for surface seismic (Zhang et al., 2001)

- second order approximation based on paraxial ray-theory
- central ray is non-zero offset
  ➥ expansion points ($\vec{x}_S$, $\vec{x}_G$) for each simulated source and receiver pair

CRS approach for VSP geometry

Finite-offset (FO) 2D CRS stack theory initially introduced for surface seismic (Zhang et al., 2001)

- second order approximation based on paraxial ray-theory
- central ray is non-zero offset
  ➥ expansion points ($\vec{x}_S$, $\vec{x}_G$) for each simulated source and receiver pair
- FO CRS operator depends on five parameters

CRS approach for VSP geometry

Finite-offset (FO) 2D CRS stack theory initially introduced for surface seismic (Zhang et al., 2001)

- second order approximation based on paraxial ray-theory
- central ray is non-zero offset
  ➥ expansion points $(\vec{x}_S, \vec{x}_G)$ for each simulated source and receiver pair
- FO CRS operator depends on five parameters
  ➥ multi-dimensional optimization problem

CRS approach for VSP geometry

Finite-offset (FO) 2D CRS stack theory initially introduced for surface seismic (Zhang et al., 2001)

- second order approximation based on paraxial ray-theory
- central ray is non-zero offset
  ➥ expansion points ($\vec{x}_S$, $\vec{x}_G$) for each simulated source and receiver pair
- FO CRS operator depends on five parameters
  ➥ multi-dimensional optimization problem
- geometrical explanation of stacking parameters

CRS approach for VSP geometry

Finite-offset (FO) 2D CRS stack theory initially introduced for surface seismic (Zhang et al., 2001)

- second order approximation based on paraxial ray-theory
- central ray is non-zero offset
  ➥ expansion points $(\vec{x}_S, \vec{x}_G)$ for each simulated source and receiver pair
- FO CRS operator depends on five parameters
  ➥ multi-dimensional optimization problem
- geometrical explanation of stacking parameters
  ➥ hypothetical wavefronts, in vicinity of sources and receivers assuming:

CRS approach for VSP geometry

Finite-offset (FO) 2D CRS stack theory initially introduced for surface seismic (Zhang et al., 2001)

- second order approximation based on paraxial ray-theory
- central ray is non-zero offset
  ➥ expansion points ($\vec{x}_S$, $\vec{x}_G$) for each simulated source and receiver pair
- FO CRS operator depends on five parameters
  ➥ multi-dimensional optimization problem
- geometrical explanation of stacking parameters
  ➥ hypothetical wavefronts, in vicinity of sources and receivers assuming:
  - local isotropy

CRS approach for VSP geometry

Finite-offset (FO) 2D CRS stack theory initially introduced for surface seismic (Zhang et al., 2001)

- second order approximation based on paraxial ray-theory
- central ray is non-zero offset
  ➥ expansion points $(\vec{x}_S, \vec{x}_G)$ for each simulated source and receiver pair
- FO CRS operator depends on five parameters
  ➥ multi-dimensional optimization problem
- geometrical explanation of stacking parameters
  ➥ hypothetical wavefronts, in vicinity of sources and receivers assuming:
  - local isotropy
  - local homogeneity

CRS approach for VSP geometry

Finite-offset (FO) 2D CRS stack theory initially introduced for surface seismic (Zhang et al., 2001)

- second order approximation based on paraxial ray-theory
- central ray is non-zero offset
  ➥ expansion points ($\vec{x}_S$, $\vec{x}_G$) for each simulated source and receiver pair
- FO CRS operator depends on five parameters
  ➥ multi-dimensional optimization problem
- geometrical explanation of stacking parameters
  ➥ hypothetical wavefronts, in vicinity of sources and receivers assuming:
  - local isotropy
  - local homogeneity
  - known velocities

CRS approach for VSP geometry

Finite-offset (FO) 2D CRS stack theory initially introduced for surface seismic (Zhang et al., 2001)

- second order approximation based on paraxial ray-theory
- central ray is non-zero offset
  ➥ expansion points ($\vec{x}_S$, $\vec{x}_G$) for each simulated source and receiver pair
- FO CRS operator depends on five parameters
  ➥ multi-dimensional optimization problem
- geometrical explanation of stacking parameters
  ➥ hypothetical wavefronts, in vicinity of sources and receivers assuming:
  - local isotropy
  - local homogeneity
  - known velocities ➥ calibration required

VSP measurement configuration

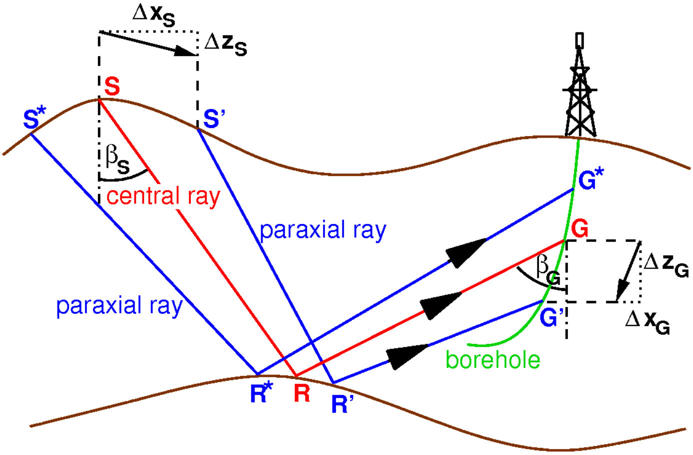

S and *G* are the positions of $\vec{x}_S$ and $\vec{x}_G$, respectively

CRS Operator for arbitrary geometry

CRS Operator for arbitrary geometry

$$
\begin{aligned}
\tau_{\mathrm{hyp}}^2 \;=\; & \left(\tau_0 + \frac{\sin\beta_S}{v_S}\,\Delta x_S - \frac{\cos\beta_S}{v_S}\,\Delta z_S + \frac{\sin\beta_G}{v_G}\,\Delta x_G - \frac{\cos\beta_G}{v_G}\,\Delta z_G \right)^2 \\
+ & \;\; \tau_0\, A B^{-1}\, (\Delta x_S - \Delta z_S \tan\beta_S)^2 \\
+ & \;\; \tau_0\, D B^{-1}\, (\Delta x_G - \Delta z_G \tan\beta_G)^2 \\
- & \;\; 2\,\tau_0\, B^{-1}\, (\Delta x_S - \Delta z_S \tan\beta_S)\,(\Delta x_G - \Delta z_G \tan\beta_G)\,.
\end{aligned}
$$

CRS Operator for arbitrary geometry

$$
\begin{aligned}
\tau_{\mathrm{hyp}}^2 \;=\; & \left(\tau_0 + \frac{\sin\beta_S}{v_S}\Delta x_S - \frac{\cos\beta_S}{v_S}\Delta z_S + \frac{\sin\beta_G}{v_G}\Delta x_G - \frac{\cos\beta_G}{v_G}\Delta z_G \right)^2 \\
+ \; & \tau_0\, AB^{-1}\, (\Delta x_S - \Delta z_S \tan\beta_S)^2 \\
+ \; & \tau_0\, DB^{-1}\, (\Delta x_G - \Delta z_G \tan\beta_G)^2 \\
- \; & 2\,\tau_0\, B^{-1}\, (\Delta x_S - \Delta z_S \tan\beta_S)\,(\Delta x_G - \Delta z_G \tan\beta_G)\,.
\end{aligned}
$$

- τ_0 : traveltime of central FO ray

CRS Operator for arbitrary geometry

$$
\begin{aligned}
\tau_{\text{hyp}}^2 \quad = \quad & \left(\tau_0 + \frac{\sin\beta_S}{v_S}\,\Delta x_S - \frac{\cos\beta_S}{v_S}\,\Delta z_S + \frac{\sin\beta_G}{v_G}\,\Delta x_G - \frac{\cos\beta_G}{v_G}\,\Delta z_G \right)^2 \\
& + \quad \tau_0\, AB^{-1}\, (\Delta x_S - \Delta z_S \tan\beta_S)^2 \\
& + \quad \tau_0\, DB^{-1}\, (\Delta x_G - \Delta z_G \tan\beta_G)^2 \\
& - \quad 2\,\tau_0\, B^{-1}\, (\Delta x_S - \Delta z_S \tan\beta_S)\, (\Delta x_G - \Delta z_G \tan\beta_G)\,.
\end{aligned}
$$

- τ_0 : traveltime of central FO ray
- $\Delta x_S, \Delta z_S, \Delta x_G, \Delta z_G$: horizontal and vertical offsets

CRS Operator for arbitrary geometry

$$
\begin{aligned}
\tau_{\text{hyp}}^2 \quad = \quad & \left(\tau_0 + \frac{\sin\beta_S}{v_S}\Delta x_S - \frac{\cos\beta_S}{v_S}\Delta z_S + \frac{\sin\beta_G}{v_G}\Delta x_G - \frac{\cos\beta_G}{v_G}\Delta z_G \right)^2 \\
+ \quad & \tau_0\, AB^{-1}\, (\Delta x_S - \Delta z_S \tan\beta_S)^2 \\
+ \quad & \tau_0\, DB^{-1}\, (\Delta x_G - \Delta z_G \tan\beta_G)^2 \\
- \quad & 2\,\tau_0\, B^{-1}\, (\Delta x_S - \Delta z_S \tan\beta_S)\, (\Delta x_G - \Delta z_G \tan\beta_G)\,.
\end{aligned}
$$

- τ_0 : traveltime of central FO ray
- $\Delta x_S, \Delta z_S, \Delta x_G, \Delta z_G$: horizontal and vertical offsets
- v_S, v_G : velocities in the vicinity of $\vec{x}_S$ and $\vec{x}_G$

CRS Operator for arbitrary geometry

$$
\begin{aligned}
\tau_{\mathrm{hyp}}^2 \quad = \quad & \left(\tau_0 + \frac{\sin\beta_S}{v_S}\Delta x_S - \frac{\cos\beta_S}{v_S}\Delta z_S + \frac{\sin\beta_G}{v_G}\Delta x_G - \frac{\cos\beta_G}{v_G}\Delta z_G \right)^2 \\
+ \quad & \tau_0\, AB^{-1}\, (\Delta x_S - \Delta z_S \tan\beta_S)^2 \\
+ \quad & \tau_0\, DB^{-1}\, (\Delta x_G - \Delta z_G \tan\beta_G)^2 \\
- \quad & 2\,\tau_0\, B^{-1}\, (\Delta x_S - \Delta z_S \tan\beta_S)\, (\Delta x_G - \Delta z_G \tan\beta_G)\,.
\end{aligned}
$$

- τ_0 : traveltime of central FO ray
- $\Delta x_S, \Delta z_S, \Delta x_G, \Delta z_G$: horizontal and vertical offsets
- v_S, v_G : velocities in the vicinity of $\vec{x}_S$ and $\vec{x}_G$
- β_S, β_G : emergence angles of central ray

CRS Operator for arbitrary geometry

$$
\begin{aligned}
\tau_{\text{hyp}}^2 \quad = \quad & \left(\tau_0 + \frac{\sin\beta_S}{v_S}\Delta x_S - \frac{\cos\beta_S}{v_S}\Delta z_S + \frac{\sin\beta_G}{v_G}\Delta x_G - \frac{\cos\beta_G}{v_G}\Delta z_G \right)^2 \\
+ \quad & \tau_0 \, AB^{-1} \, (\Delta x_S - \Delta z_S \tan\beta_S)^2 \\
+ \quad & \tau_0 \, DB^{-1} \, (\Delta x_G - \Delta z_G \tan\beta_G)^2 \\
- \quad & 2\,\tau_0 \, B^{-1} \, (\Delta x_S - \Delta z_S \tan\beta_S)\,(\Delta x_G - \Delta z_G \tan\beta_G)\,.
\end{aligned}
$$

- τ_0 : traveltime of central FO ray
- $\Delta x_S, \Delta z_S, \Delta x_G, \Delta z_G$: horizontal and vertical offsets
- v_S, v_G : velocities in the vicinity of $\vec{x}_S$ and $\vec{x}_G$
- β_S, β_G : emergence angles of central ray
- DB^{-1}, AB^{-1}, B^{-1} : composites of elements of ray-propagator matrix

A look at multi-coverage walkover data

A look at multi-coverage walkover data

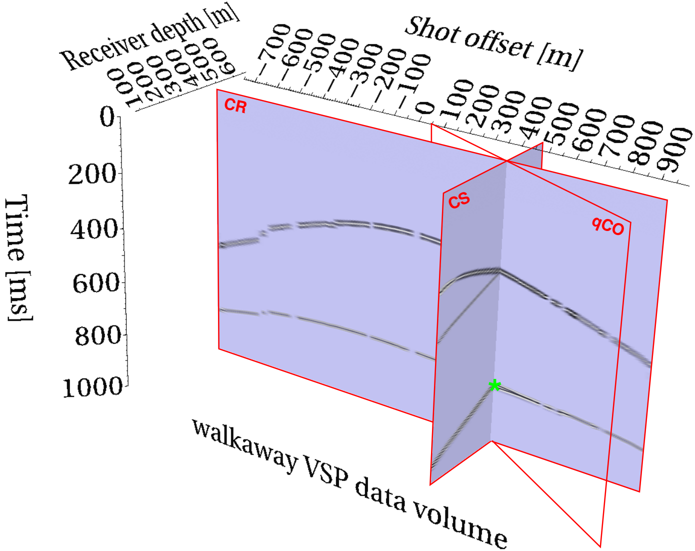

Calibration of CRS attributes

Calibration of CRS attributes

Stacking parameters are converted to wavefield attributes by using tuned velocities.

Calibration of CRS attributes

Stacking parameters are converted to wavefield attributes by using tuned velocities.

- inaccurate velocities ⇔ incorrect attributes

Calibration of CRS attributes

Stacking parameters are converted to wavefield attributes by using tuned velocities.

- inaccurate velocities $\Leftrightarrow$ incorrect attributes
- conventional way: checkshot inversion

Calibration of CRS attributes

Stacking parameters are converted to wavefield attributes by using tuned velocities.

- inaccurate velocities $\Leftrightarrow$ incorrect attributes
- conventional way: checkshot inversion often too inaccurate!

Calibration of CRS attributes

Stacking parameters are converted to wavefield attributes by using tuned velocities.

- inaccurate velocities $\Leftrightarrow$ incorrect attributes
- conventional way: checkshot inversion
  often too inaccurate!
- alternatively: CRS analysis of downgoing waves

Calibration of CRS attributes

Stacking parameters are converted to wavefield attributes by using tuned velocities.

- inaccurate velocities ⇔ incorrect attributes
- conventional way: checkshot inversion often too inaccurate!
- alternatively: CRS analysis of downgoing waves

Assumption:

Calibration of CRS attributes

Stacking parameters are converted to wavefield attributes by using tuned velocities.

- inaccurate velocities $\Leftrightarrow$ incorrect attributes
- conventional way: checkshot inversion
  often too inaccurate!
- alternatively: CRS analysis of downgoing waves

Assumption:

- velocities virtually constant within paraxial vicinity

Calibration of CRS attributes

Stacking parameters are converted to wavefield attributes by using tuned velocities.

- inaccurate velocities $\Leftrightarrow$ incorrect attributes
- conventional way: checkshot inversion
  often too inaccurate!
- alternatively: CRS analysis of downgoing waves

Assumption:

- velocities virtually constant within paraxial vicinity
  (already inherent assumption of CRS method)

Calibration of CRS attributes

Stacking parameters are converted to wavefield attributes by using tuned velocities.

- inaccurate velocities ⇔ incorrect attributes
- conventional way: checkshot inversion
  often too inaccurate!
- alternatively: CRS analysis of downgoing waves

Assumption:

- velocities virtually constant within paraxial vicinity
  (already inherent assumption of CRS method)
  ➥ length of slowness vector $|\vec{p}|$ independent of incidence angle

Calibration strategy

Calibration strategy

- VSP data provides only one slowness component:

Calibration strategy

- VSP data provides only one slowness component: slowness component p_t tangent to well

Calibration strategy

- VSP data provides only one slowness component: slowness component p_t tangent to well
  ➥ in general insufficient to determine $|\vec{p}|$

Calibration strategy

- VSP data provides only one slowness component: slowness component p_t tangent to well
  ➥ in general insufficient to determine $|\vec{p}|$
- special case: walkover VSP

Calibration strategy

- VSP data provides only one slowness component: slowness component p_t tangent to well
  ➥ in general insufficient to determine $|\vec{p}|$
- special case: walkover VSP
  - p_t of downgoing rays varies with source position $\vec{x}_S$

Calibration strategy

- VSP data provides only one slowness component: slowness component p_t tangent to well
  ➥ in general insufficient to determine $|\vec{p}|$
- special case: walkover VSP
  - p_t of downgoing rays varies with source position $\vec{x}_S$
  - a ray tangent to well at receiver $\vec{x}_G$ is very likely

Calibration strategy

- VSP data provides only one slowness component: slowness component p_t tangent to well
  ➥ in general insufficient to determine $|\vec{p}|$
- special case: walkover VSP
  - p_t of downgoing rays varies with source position $\vec{x}_S$
  - a ray tangent to well at receiver $\vec{x}_G$ is very likely there: naturally $p_t \equiv |\vec{p}|$

Calibration strategy

- VSP data provides only one slowness component: slowness component p_t tangent to well
  ➥ in general insufficient to determine $|\vec{p}|$
- special case: walkover VSP
  - p_t of downgoing rays varies with source position $\vec{x}_S$
  - a ray tangent to well at receiver $\vec{x}_G$ is very likely there: naturally $p_t \equiv |\vec{p}|$
- Strategy

Calibration strategy

- VSP data provides only one slowness component: slowness component p_t tangent to well
  ➥ in general insufficient to determine $|\vec{p}|$
- special case: walkover VSP
  - p_t of downgoing rays varies with source position $\vec{x}_S$
  - a ray tangent to well at receiver $\vec{x}_G$ is very likely there: naturally $p_t \equiv |\vec{p}|$
- Strategy
  - identify downgoing direct P and/or S arrivals

Calibration strategy

- VSP data provides only one slowness component: slowness component p_t tangent to well
  ➥ in general insufficient to determine $|\vec{p}|$
- special case: walkover VSP
  - p_t of downgoing rays varies with source position $\vec{x}_S$
  - a ray tangent to well at receiver $\vec{x}_G$ is very likely there: naturally $p_t \equiv |\vec{p}|$
- Strategy
  - identify downgoing direct P and/or S arrivals
  - calculate $p_t\left(\vec{x}_S, \vec{x}_G\right)$ $\forall$ sources S and receivers G

Calibration strategy

- VSP data provides only one slowness component: slowness component p_t tangent to well
  ➥ in general insufficient to determine $|\vec{p}|$
- special case: walkover VSP
  - p_t of downgoing rays varies with source position $\vec{x}_S$
  - a ray tangent to well at receiver $\vec{x}_G$ is very likely there: naturally $p_t \equiv |\vec{p}|$
- Strategy
  - identify downgoing direct P and/or S arrivals
  - calculate $p_t\left(\vec{x}_S, \vec{x}_G\right)$ $\forall$ sources S and receivers G
  - for each G, search maximum of $p_t\left(\vec{x}_S, \vec{x}_G = \text{const}\right)$

Calibration strategy

- VSP data provides only one slowness component: slowness component p_t tangent to well
  ➥ in general insufficient to determine $|\vec{p}|$
- special case: walkover VSP
  - p_t of downgoing rays varies with source position $\vec{x}_S$
  - a ray tangent to well at receiver $\vec{x}_G$ is very likely there: naturally $p_t \equiv |\vec{p}|$
- Strategy
  - identify downgoing direct P and/or S arrivals
  - calculate $p_t\left(\vec{x}_S, \vec{x}_G\right)$ $\forall$ sources S and receivers G
  - for each G, search maximum of $p_t\left(\vec{x}_S, \vec{x}_G = \text{const}\right)$

➥ searched-for velocity $v\left(\vec{x}_G\right) = \max\left\{p_t\left(\vec{x}_S; \vec{x}_G\right)\right\}^{-1}$

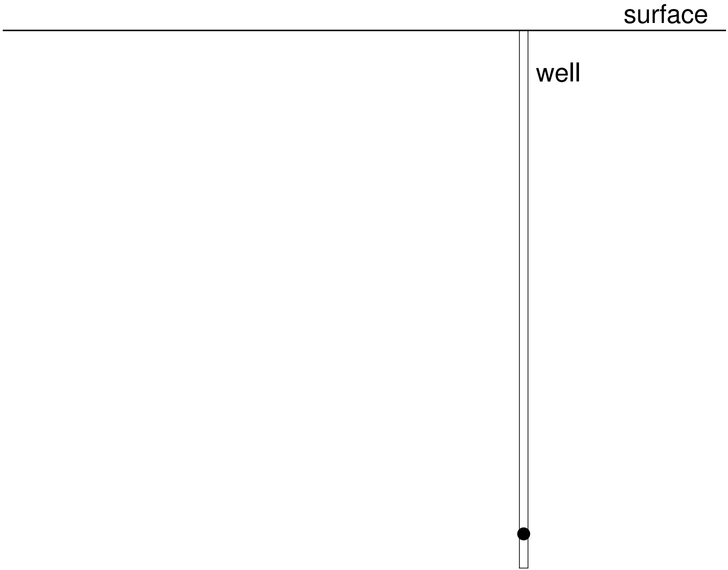
surface
well

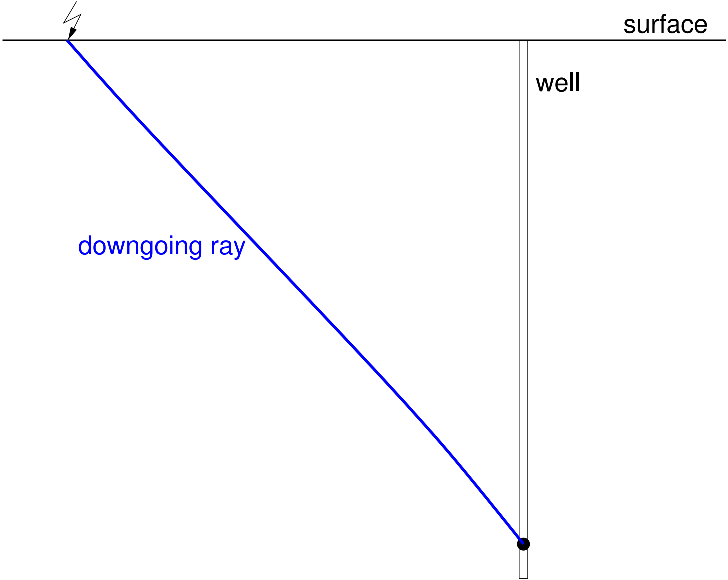
surface
well
downgoing ray

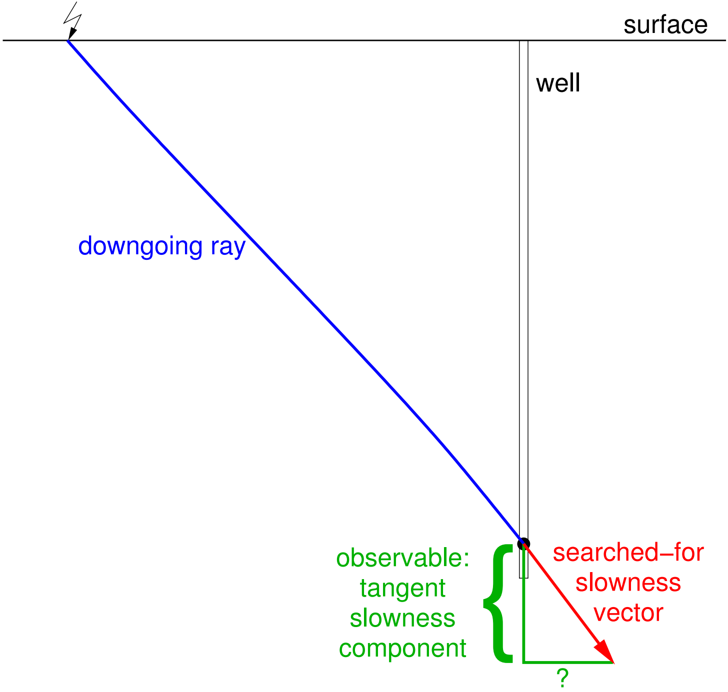
surface
well
downgoing ray
observable:
tangent
slowness
component
searched–for
slowness
vector
?

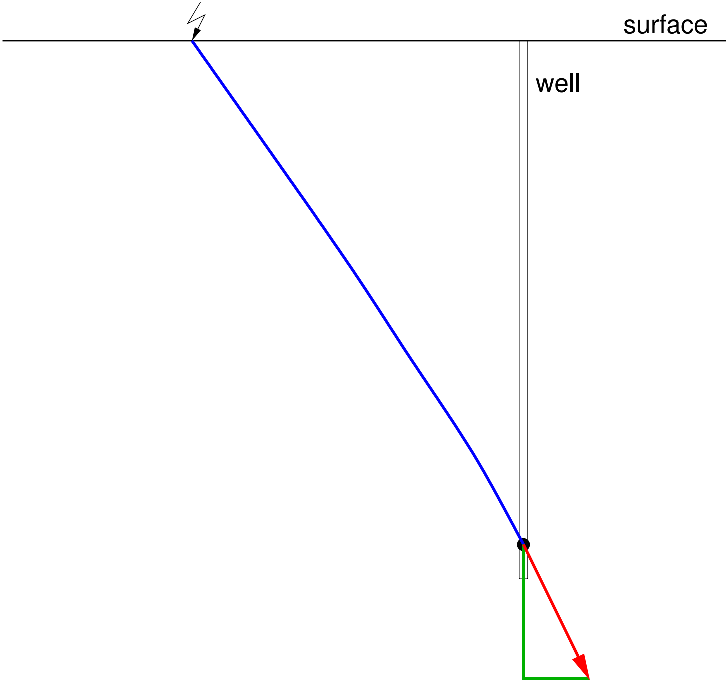
surface
well

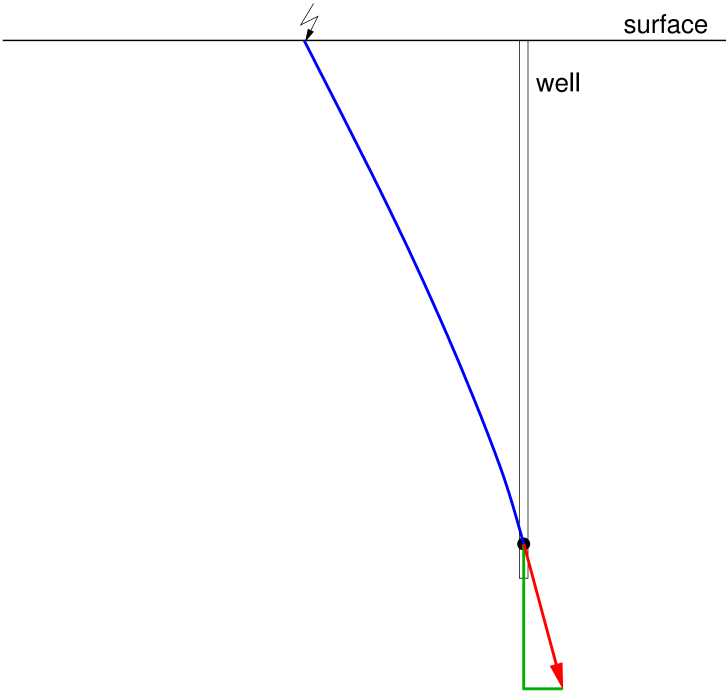
surface
well

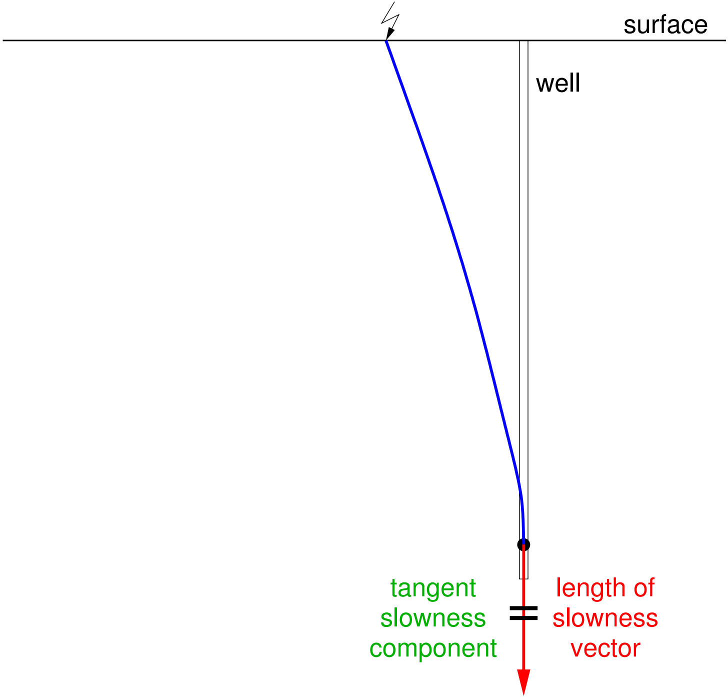
surface
well
tangent slowness component
=
length of slowness vector

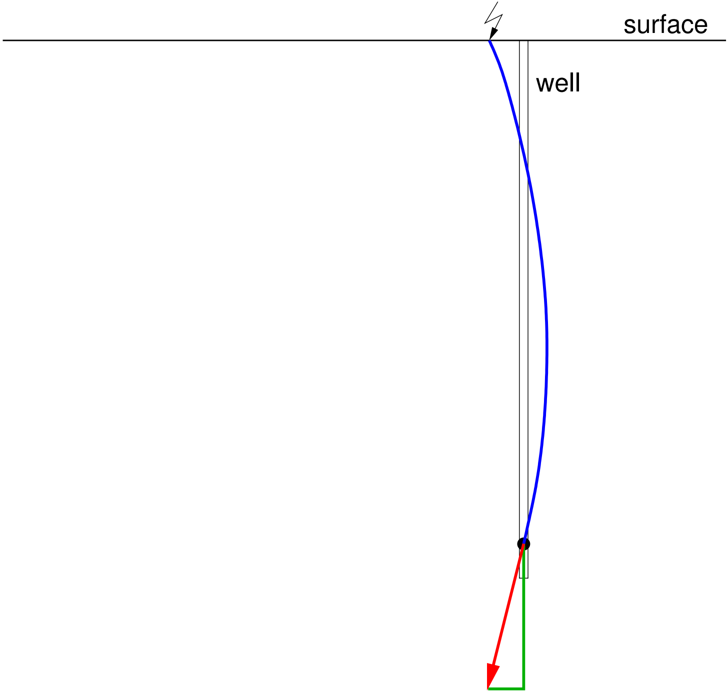
surface
well

Application of tuned velocities

Application of tuned velocities

- separate calibration for P- and S-waves

Application of tuned velocities

- separate calibration for P- and S-waves
- velocity v_G is property of receiver position

Application of tuned velocities

- separate calibration for P- and S-waves
- velocity v_G is property of receiver position
  ➥ applicable to also calibrate *reflected* waves

Application of tuned velocities

- separate calibration for P- and S-waves
- velocity v_G is property of receiver position
  ➥ applicable to also calibrate *reflected* waves
- Geometric interpretation provides

Application of tuned velocities

- separate calibration for P- and S-waves
- velocity v_G is property of receiver position
  ➥ applicable to also calibrate *reflected* waves
- Geometric interpretation provides
  - emergence angles

Application of tuned velocities

- separate calibration for P- and S-waves
- velocity v_G is property of receiver position
  ➥ applicable to also calibrate *reflected* waves
- Geometric interpretation provides
  - emergence angles
  - wavefront curvatures

Application of tuned velocities

- separate calibration for P- and S-waves
- velocity v_G is property of receiver position
  ➥ applicable to also calibrate *reflected* waves
- Geometric interpretation provides
  - emergence angles
  - wavefront curvatures
- suited for

Application of tuned velocities

- separate calibration for P- and S-waves
- velocity v_G is property of receiver position
  ➥ applicable to also calibrate *reflected* waves
- Geometric interpretation provides
  - emergence angles
  - wavefront curvatures
- suited for
  - wavefield decomposition

Application of tuned velocities

- separate calibration for P- and S-waves
- velocity v_G is property of receiver position
  ➥ applicable to also calibrate *reflected* waves
- Geometric interpretation provides
  - emergence angles
  - wavefront curvatures
- suited for
  - wavefield decomposition ➥ data example

Application of tuned velocities

- separate calibration for P- and S-waves
- velocity v_G is property of receiver position
  ➥ applicable to also calibrate *reflected* waves
- Geometric interpretation provides
  - emergence angles
  - wavefront curvatures
- suited for
  - wavefield decomposition ➥ data example
  - redatuming

Application of tuned velocities

- separate calibration for P- and S-waves
- velocity v_G is property of receiver position
  ➥ applicable to also calibrate *reflected* waves
- Geometric interpretation provides
  - emergence angles
  - wavefront curvatures
- suited for
  - wavefield decomposition ➥ data example
  - redatuming
  - inversion

Application of tuned velocities

- separate calibration for P- and S-waves
- velocity v_G is property of receiver position
  ➥ applicable to also calibrate *reflected* waves
- Geometric interpretation provides
  - emergence angles
  - wavefront curvatures
- suited for
  - wavefield decomposition ➥ data example
  - redatuming
  - inversion
- strategy also suited for deviated wells

Model and survey geometry

Model and survey geometry

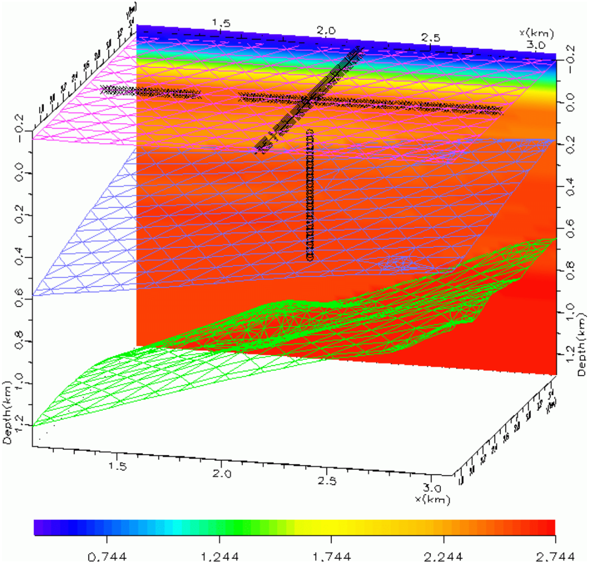

P-wave velocity [km/s]

Model and survey geometry

Modeling:

Model and survey geometry

Modeling:

- wavefront construction method

Model and survey geometry

Modeling:

- wavefront construction method
- direct P, reflected PP & SS, converted PS

Model and survey geometry

Modeling:

- wavefront construction method
- direct P, reflected PP & SS, converted PS
- 3D wave propagation

Model and survey geometry

Modeling:

- wavefront construction method
- direct P, reflected PP & SS, converted PS
- 3D wave propagation
- two walkover lines, 100 shots each

Model and survey geometry

Modeling:

- wavefront construction method
- direct P, reflected PP & SS, converted PS
- 3D wave propagation
- two walkover lines, 100 shots each
- 40 three-component receiver levels

Model and survey geometry

Modeling:

- wavefront construction method
- direct P, reflected PP & SS, converted PS
- 3D wave propagation
- two walkover lines, 100 shots each
- 40 three-component receiver levels
- 2D approach sufficiently accurate for calibration

Model and survey geometry

Model and survey geometry

convenient CRS parameter: emergence angle

Model and survey geometry

convenient CRS parameter: emergence angle

➥ tangency $\equiv$ zero angle

Model and survey geometry

convenient CRS parameter: emergence angle

➥ tangency ≡ zero angle

Expected behavior:

Model and survey geometry

convenient CRS parameter: emergence angle

➥ tangency ≡ zero angle

Expected behavior:

- over-estimated velocity

Model and survey geometry

convenient CRS parameter: emergence angle

➥ tangency ≡ zero angle

Expected behavior:

- over-estimated velocity
  zero angle smeared over large offset range

Model and survey geometry

convenient CRS parameter: emergence angle

➥ tangency ≡ zero angle

Expected behavior:

- over-estimated velocity
  zero angle smeared over large offset range
- under-estimated velocity

Model and survey geometry

convenient CRS parameter: emergence angle

➥ tangency ≡ zero angle

Expected behavior:

- over-estimated velocity
  zero angle smeared over large offset range
- under-estimated velocity
  zero angle never occurs

Model and survey geometry

convenient CRS parameter: emergence angle

➥ tangency ≡ zero angle

Expected behavior:

- over-estimated velocity
  zero angle smeared over large offset range
- under-estimated velocity
  zero angle never occurs
- correct velocity

Model and survey geometry

convenient CRS parameter: emergence angle

➥ tangency ≡ zero angle

Expected behavior:

- over-estimated velocity
  zero angle smeared over large offset range
- under-estimated velocity
  zero angle never occurs
- correct velocity
  well-localized minimum at zero angle

Calibration using checkshot inversion

Calibration using checkshot inversion

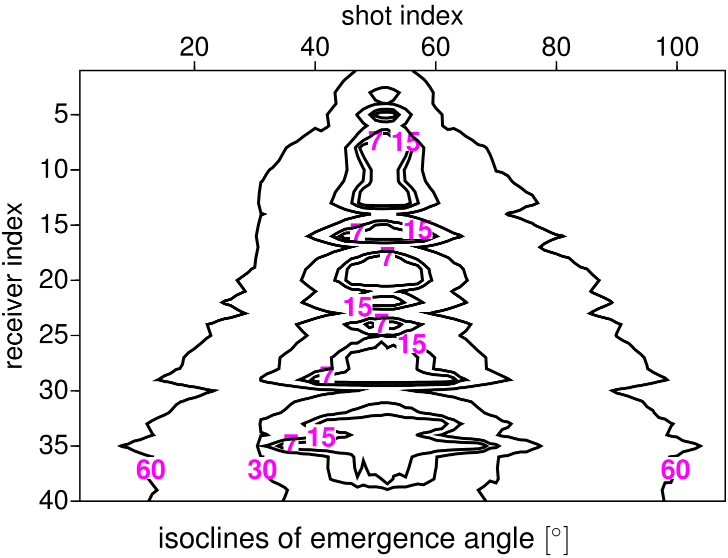

Calibration with initial model

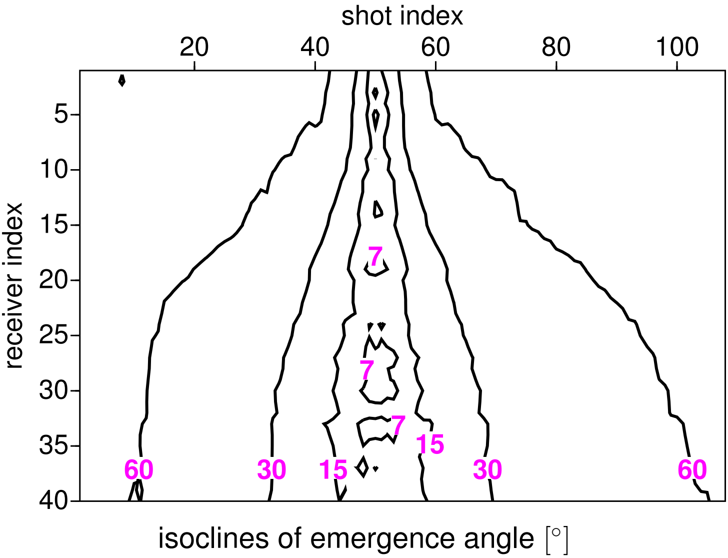

Calibration with corrected model

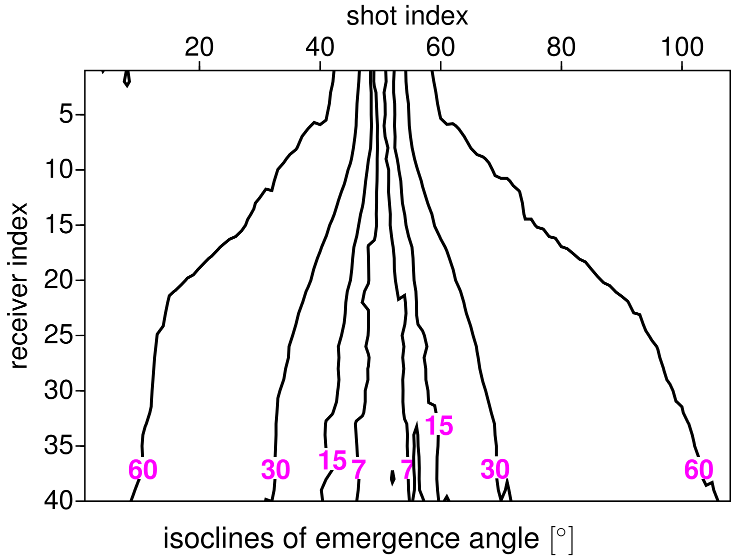

Forward-modeled angles

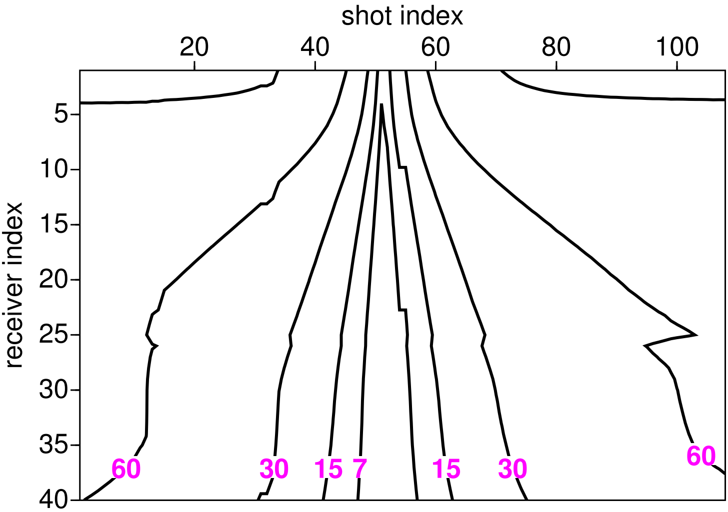

isoclines of emergence angle [°]

1D velocity curves along well

1D velocity curves along well

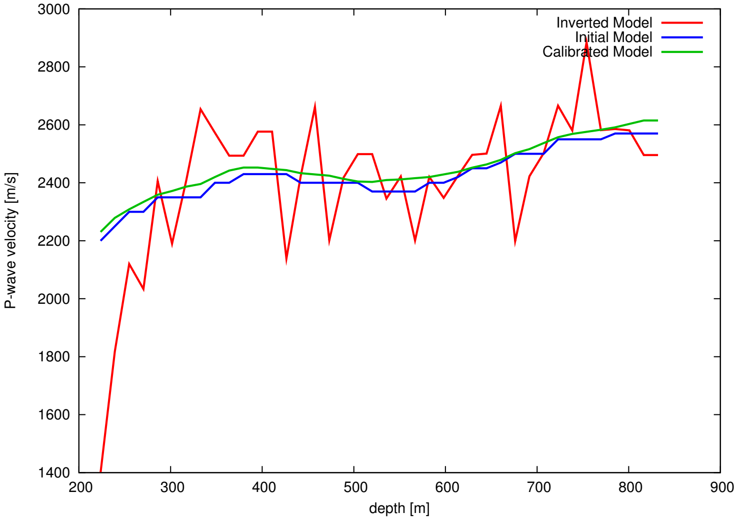

CRS-based wavefield decomposition

CRS-based wavefield decomposition

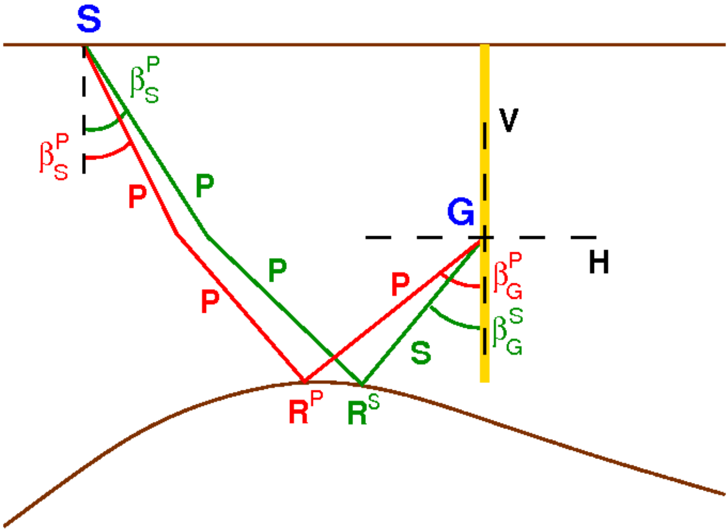

Components (V,H) prior to rotation

CRS-based wavefield decomposition

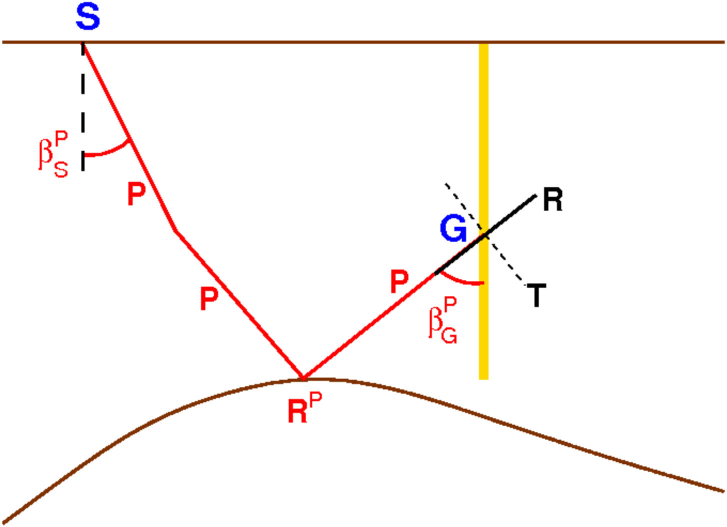

Components (R,T) after rotation by β_G^P – R is strong

CRS-based wavefield decomposition

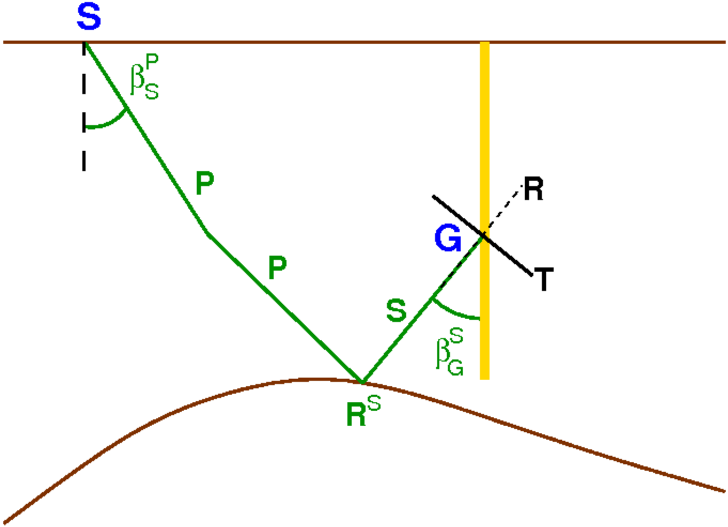

Components (R,T) after rotation by β_G^S – T is strong

Five CS gathers prior to rotation

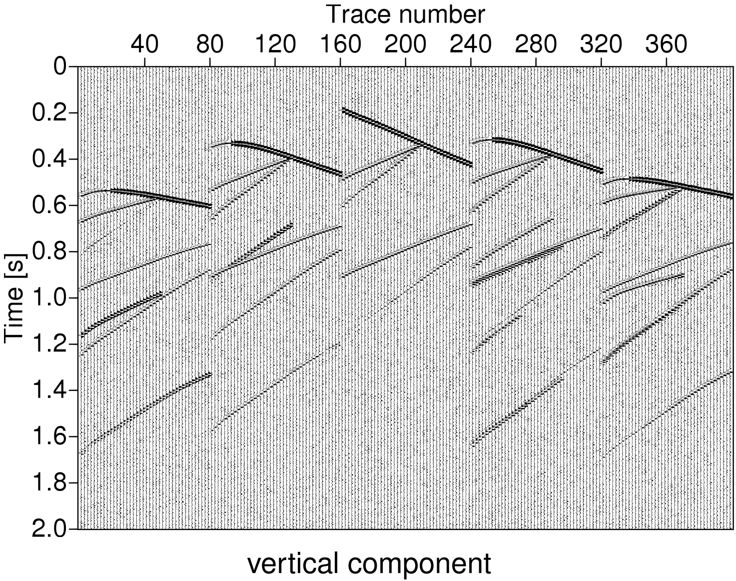

Five CS gathers prior to rotation

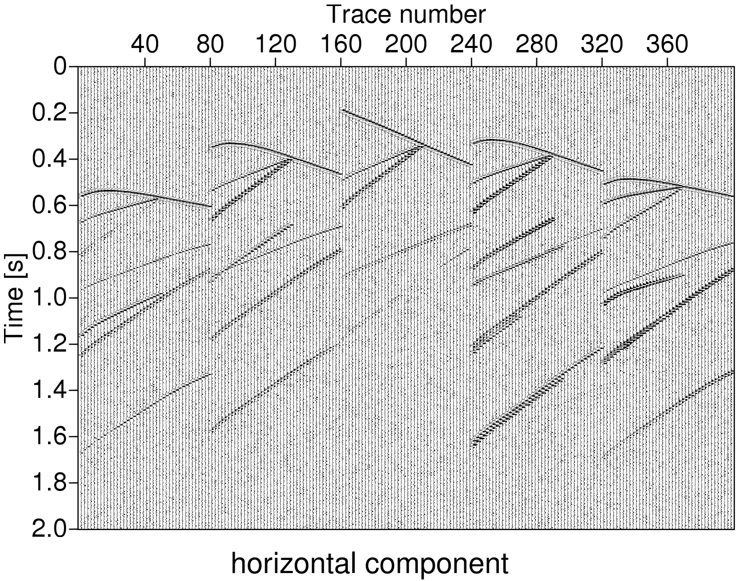

Five CS gathers after decomposition

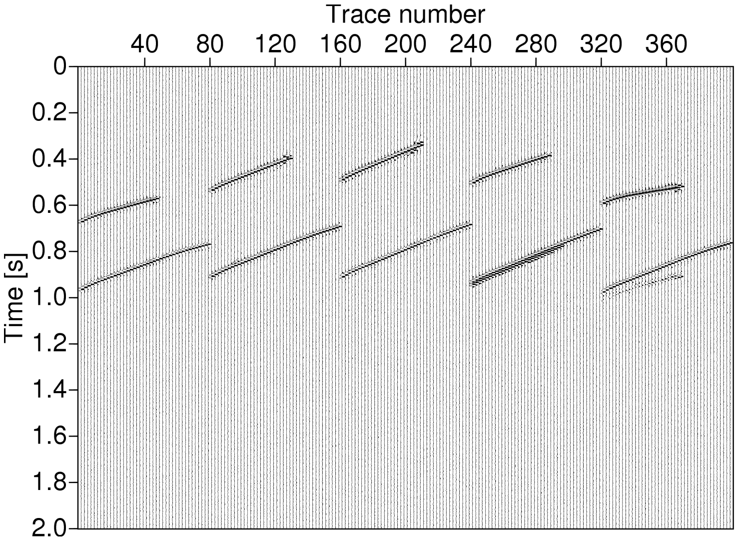

radial orientation using β_G^P

Five CS gathers after decomposition

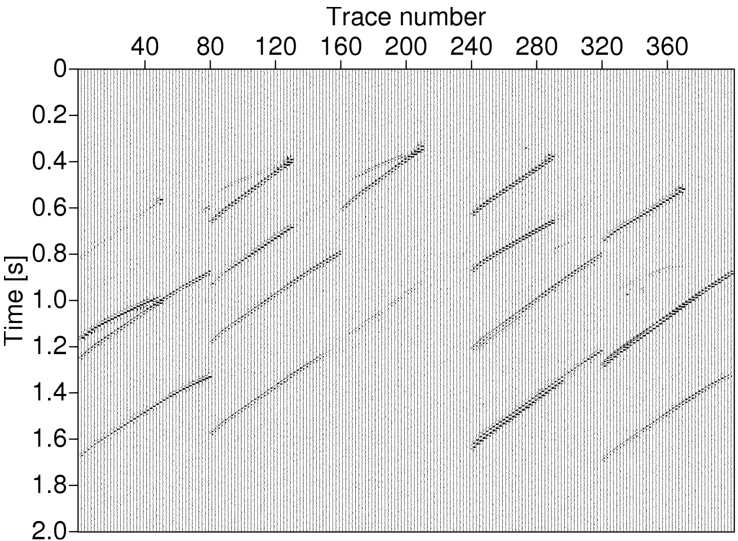

transverse orientation using β_G^S

Conclusions & outlook

Conclusions & outlook

Calibration of CRS attributes

Conclusions & outlook

Calibration of CRS attributes

- high sensitivity to inaccurate velocity

Conclusions & outlook

Calibration of CRS attributes

- high sensitivity to inaccurate velocity
- simple criterion to determine tuned velocities

Conclusions & outlook

Calibration of CRS attributes

- high sensitivity to inaccurate velocity
- simple criterion to determine tuned velocities
- readily applicable to 3D data and deviated wells

Conclusions & outlook

Calibration of CRS attributes

- high sensitivity to inaccurate velocity
- simple criterion to determine tuned velocities
- readily applicable to 3D data and deviated wells
- reliable *geometrical* CRS attributes for

Conclusions & outlook

Calibration of CRS attributes

- high sensitivity to inaccurate velocity
- simple criterion to determine tuned velocities
- readily applicable to 3D data and deviated wells
- reliable *geometrical* CRS attributes for
  - wavefield decomposition

Conclusions & outlook

Calibration of CRS attributes

- high sensitivity to inaccurate velocity
- simple criterion to determine tuned velocities
- readily applicable to 3D data and deviated wells
- reliable *geometrical* CRS attributes for
  - wavefield decomposition
  - redatuming

Conclusions & outlook

Calibration of CRS attributes

- high sensitivity to inaccurate velocity
- simple criterion to determine tuned velocities
- readily applicable to 3D data and deviated wells
- reliable *geometrical* CRS attributes for
  - wavefield decomposition
  - redatuming
  - inversion, e. g. stereo tomography

Conclusions & outlook

Calibration of CRS attributes

- high sensitivity to inaccurate velocity
- simple criterion to determine tuned velocities
- readily applicable to 3D data and deviated wells
- reliable *geometrical* CRS attributes for
  - wavefield decomposition
  - redatuming
  - inversion, e. g. stereo tomography
  - …

Conclusions & outlook

Calibration of CRS attributes

- high sensitivity to inaccurate velocity
- simple criterion to determine tuned velocities
- readily applicable to 3D data and deviated wells
- reliable *geometrical* CRS attributes for
  - wavefield decomposition
  - redatuming
  - inversion, e. g. stereo tomography
  - ...
- possible combination with hodogram analysis

Acknowledgments

This work was kindly supported by. . .

- the sponsors of the Wave Inversion Technology (WIT) Consortium
- Paulsson Geophysical Services Inc. for providing synthetic data and tremendous assistance in questions of VSP imaging